

Design of a high-performance catalyst for CO oxidation: Au nanoparticles confined in mesoporous aluminosilicate

Jun-Hong Liu^a, Yu-Shan Chi^a, Hong-Ping Lin^b, Chung-Yuan Mou^{a,*}, Ben-Zu Wan^c

^a Department of Chemistry, National Taiwan University, Taipei 106, Taiwan

^b Department of Chemistry, National Cheng Kung University, Tainan 701, Taiwan

^c Department of Chemical Engineering, National Taiwan University, Taipei 106, Taiwan

Available online 15 July 2004

Abstract

Au nanoparticles embedded within mesoporous aluminosilicate particles have been prepared and used as catalyst for CO oxidation. In the presence of C₁₆TMAB, a stable aqueous solution of Au nanoparticles-surfactant without apparent aggregations was obtained by chemical reduction. After combining with aluminosilicates in an alkaline solution, the Au nanoparticles were mostly embedded within the mesoporous aluminosilicate particles, and the maximum loading of Au nanoparticle can reach around 36 wt.%. The diameter of Au nanoparticles in mesoporous aluminosilicates are <10 nm after calcination at 560 °C under air. In this research, the quaternary ammonium surfactants serve as dual function agents, protecting agent for Au nanoparticle and templates for mesoporous silica. When the mesoporous aluminosilicate supports are in micron-size, the highest CO conversion is only about 16% over the catalyst with gold loading, Au/SiO₂ = 8%. The conversion decreases to nearly zero at higher gold loadings due to extensive pore blocking. Reducing the dimension of mesoporous aluminosilicates to tens of nanometers makes the Au nanoparticles more accessible for CO oxidation, and the highest CO conversion reaches 70% over the catalyst with gold loading, Au/SiO₂ = 24 wt.%.

© 2004 Elsevier B.V. All rights reserved.

Keywords: Au nanoparticle; Mesoporous silica; CO oxidation; Catalysis

1. Introduction

Gold in bulk has been regarded as chemically inactive. When gold is small enough, in nanometer size, it is no longer chemically inert and performs well in several important catalytic reactions. Oxides supported Au nanoparticles exhibit interesting size-dependent catalytic properties at low temperature, in particular for CO oxidation [1]. The size effect in Au catalyzed CO oxidation is an outstanding research problem in catalysis [2–4]. It has been shown that there is an optimum size of Au nanoparticle around 3 nm [5,6] for CO oxidation. However, the underlying physical chemistry is complicated and not understood yet. The complication arises mainly from the strong effect from support [7,8]. Therefore, the method for deposition of Au nanoparticles and the kind of oxide used as support affect the catalytic activity. Nevertheless, previous preparation methods, such as precipitation or impregnation, usually lead to non-uniform distribution of sizes of gold on the supports.

At the present, there are two views with regard to the size effect of gold nanoparticle in catalysis. The first one proposes the change in electronic state in size-tuning [9]. The second one proposes that the contact between Au nanoparticle and the support is the active site for the reaction of CO and oxygen; thus, the size effect is actually about the size of the contact perimeter [6]. To follow up on the second view, Rolison showed recently that extensive contact between Au particle and support surface can be achieved with pre-formed Au nanoparticles dispersed in TiO₂ aerogel [10]. She was able to improve the catalytic activity with this catalyst design. This is a significant progress because the pre-formed gold nanoparticles can be prepared by well-developed solution methods, in which the size-control is precise.

A related but different approach would be dispersing the Au nanoparticles homogeneously inside the mesoporous materials. Since the discovery of M41S mesoporous silica synthesized using quaternary ammonium surfactants as template, the mesoporous silica have attracted considerable attention due to the potential advantages of high surface area (~1000 m²/g), tunable uniform pore size (2–30 nm), and large pore volume (400–600 cm³/g, STP).

* Corresponding author. Tel.: +886 2 33665251.

E-mail address: cymou@ntu.edu.tw (C.-Y. Mou).

We previously have designed a method for dispersing pre-formed Au nanoparticles directly inside the mesoporous MCM-41 matrix [11]. However, the catalytic activity of the resulted sample for CO oxidation is not high enough. Part of the reasons may be due to the inertness of the silica support. Moreover, it may be due to the long 1D channels of MCM-41 blocked by Au nanoparticles. Because the pore of mesostructure MCM-41 is one-dimensional, any internal blockage will seal off the nanoparticle trapped inside the channel for the reaction of CO oxidation. Therefore, compared to the aerogel support, with interconnected mesopores, the very long channels of MCM-41 is certainly a disadvantage [12] for application. Accordingly, the strategy for improving the catalyst activity then appears to be obvious. One should use nanosized MCM-41 as a support for gold. The reactant molecules could avoid a long journey through the channels and possible obstruction. Nanosized architecture domain of mesoporous materials may act as high-performance catalyst support instead of the common MCM-41, which is in micrometer size usually.

To achieve this goal, some problems have to be solved. First, uniform nanoparticles of Au are to be prepared. Then one needs a good method for dispersing Au nanoparticles homogeneously inside the mesoporous aluminosilicate particles. Finally, one needs to make the size of the mesoporous silica particles as small as possible to have high accessibility for facilitating better transports of reactants. In the past, Ghosh and Zhu prepared Au@mesoporous silica by using chemical vapor deposition (CVD) with expensive Au complex precursor [13–15], in order to have uniform distribution of nanogold inside mesopores. However, they did not study the catalytic activity of their mesoporous materials.

In this paper, we described a one-pot synthetic method, by which the C_{16} TMAB surfactant acts as a agent for protecting Au nanoparticles and as a mesostructural template for preparing nanosized MCM-41 aluminosilicates. Moreover, only cheap chloroauric acid was used as Au precursor. Thus, the as-prepared sample would have Au nanoparticles embedded within the nanosized MCM-41 aluminosilicate particles. The principle involved in designing such small particles of MCM-41 will be briefly described. We then employed this uniquely designed catalyst system for the CO oxidation system.

2. Experimental sections

2.1. Materials

The silica source is sodium silicate (27% SiO_2 , 14% NaOH) from Aldrich, and the source of aluminum is sodium aluminate ($NaAlO_2$) from Riedel-de Haën. The chloroauric acid ($HAuCl_4 \cdot 3H_2O$) and sodium borohydride ($NaBH_4$) were purchased from Acrôs. The templating agents, alkyltrimethylammonium bromide (C_n TMAB, $n = 12$ or 16), were purchased from Acrôs. Sulfuric acid

(H_2SO_4 , 96%) is from Merck. All the chemicals were used directly without further purification.

2.2. Synthesis

2.2.1. Au@ C_n TMAB aqueous solution

An aqueous solution of chloroauric acid was mixed with alkyltrimethylammonium bromide to give an orange colored solution. A proper amount of aqueous $NaBH_4$ solution as reducing agent was added drop-wise at $40^\circ C$ to the chloroauric solution. The solution color turned to dark red due to the formation of gold nanoparticles. The molar ratio of chemical components in the solution is: 1.0 C_n TAMB:(0–0.6) Au:(0–0.96) $NaBH_4$:(500–600) H_2O .

2.2.2. Au@MCM-41

For the synthesis of Au nanoparticles embedded within the micron-sized aluminosilicate MCM-41, a desired amount of sodium silicate and sodium aluminate solution was mixed with aqueous Au@ C_n TMAB solution. A red-purple colored precipitate was formed within seconds. Then, that gel-solution was neutralized by adding 1.2 M H_2SO_4 drop-wise to a pH value of about 8–10. After that, the gel solution underwent a hydrothermal reaction at $100^\circ C$ for 0–48 h. Finally, the as-synthesized material was obtained by filtration, washing with de-ionized water, and drying at $60^\circ C$. The as-synthesized product was calcined at $560^\circ C$ in air to remove the organic template, and the Au@MCM-41 catalyst was obtained. The overall molar ratio of the gel solution is 1.0 C_n TMAB:1.4 SiO_2 :0.04 $NaAlO_2$:425 H_2O .

2.2.3. Au@nanoMCM-41

For the synthesis of Au nanoparticles embedded within the nanosized aluminosilicate MCM-41 (Au@nanoMCM-41), a fast neutralization of a dilute solution of surfactant-silicate was performed according to our previous report [16]. To achieve fast nucleation, the H_2SO_4 solution was quickly poured into the alkaline solution (pH \sim 12.0) of Au@ C_n TMAB-aluminosilicate. In a very dilute solution (surfactant/ $H_2O = 1/2800$), serious aggregations of mesoporous aluminosilicate nanoparticles could be effectively reduced. The chemical composition in the solution is 1.0 C_n TMAB:5.5 SiO_2 :0.156 $NaAlO_2$:2800 H_2O .

2.3. Catalyst characterization

The X-ray powder diffraction (XRD) measurements were carried out on a Scintag X1 diffractometer with Cu $K\alpha$ radiation ($\lambda = 0.154$ nm) operated at 40 kV and 30 mA. The mean size of gold nanoparticles was estimated from the width at half maximum calculated by using Scherrer equation. The accuracy of the estimation was checked by a few TEM examinations. The N_2 adsorption–desorption isotherms were obtained at 77 K on a Micromeritics ASAP 2010 apparatus. The TEM pictures were taken on a Hitachi H7100 electron microscope operated at 75 kV or Phillips CM200 electron

microscope operated at 200 kV. For the measurements of diffuse-reflectance UV–vis spectra, a Hitachi U-3010 spectrophotometer, using BaSO₄ as reflection reference, was used.

2.4. Catalytic activity for CO oxidation

Carbon monoxide oxidation was carried out in a fused-quartz tube reactor with 0.02 g of Au@mesoporous aluminosilicates at 353 K under atmospheric pressure. Prior to catalytic reactions, the catalysts were heated to 600 °C under H₂/N₂ flow and held for 1 h, and then cooled to room temperature under N₂ flow. During the reaction, 32.7 ml/min of air and 0.33 ml/min of carbon monoxide were mixed before the inlet of the reactor. A Shimadzu GC-8A gas chromatograph with a Carboxy-2000 column was used to analyze the amount of carbon dioxide, carbon monoxide, nitrogen, and oxygen.

3. Results and discussion

Fig. 1A shows the UV–vis spectra of freshly prepared gold nanoparticle solution with C₁₆TMAB and C₁₂TMAB as surfactants. Both samples show the characteristic surface plasmon resonance absorption peak of gold nanoparticles around 520 nm. Compared to the Au@C₁₆TMAB solution,

the Au nanoparticles protected with the shorter carbon-chain C₁₂TMAB surfactant exhibit a slightly red-shifted (to 528 nm) and a broader absorption band, which indicates a larger mean particle size and more particle aggregation [17]. To examine the Au particle size, the TEM microscopic observation was performed. It was found that the sizes of Au nanoparticles are about 5–8 nm without aggregation in the Au@C₁₆TMAB sample. On the other hand, the Au nanoparticles are larger than 10 nm with fractal-shaped aggregations in the Au@C₁₂TMAB sample. The TEM observations are consistent with the results of red shift in UV–vis spectra.

Surfactant with longer carbon-chain length has higher hydrophobicity and forms more stable micelles. Therefore, C₁₆TMAB surfactant performs better as the protecting agent than C₁₂TMAB, and better dispersed gold nanoparticles are formed in the solution with C₁₆TMAB. Actually, Au@C₁₆TMAB solution can stand at least for 1 week without apparent change of gold particle size or forming aggregation. Therefore in the later sections of this research, only the more stable Au@C₁₆TMAB aqueous solution was used to prepare Au@MCM-41. With the incorporation of Au@C₁₆TMAB with aluminosilicate solution, it was found that the resulted Au@MCM-41 materials appeared in dark-red color. Fig. 2A shows the XRD pattern of the calcined Au@MCM-41. One can easily find four XRD peaks at low angle $2\theta = 1.5^\circ\text{--}8^\circ$, which indicate the well-ordered mesostructure of MCM-41. Moreover, two additional peaks

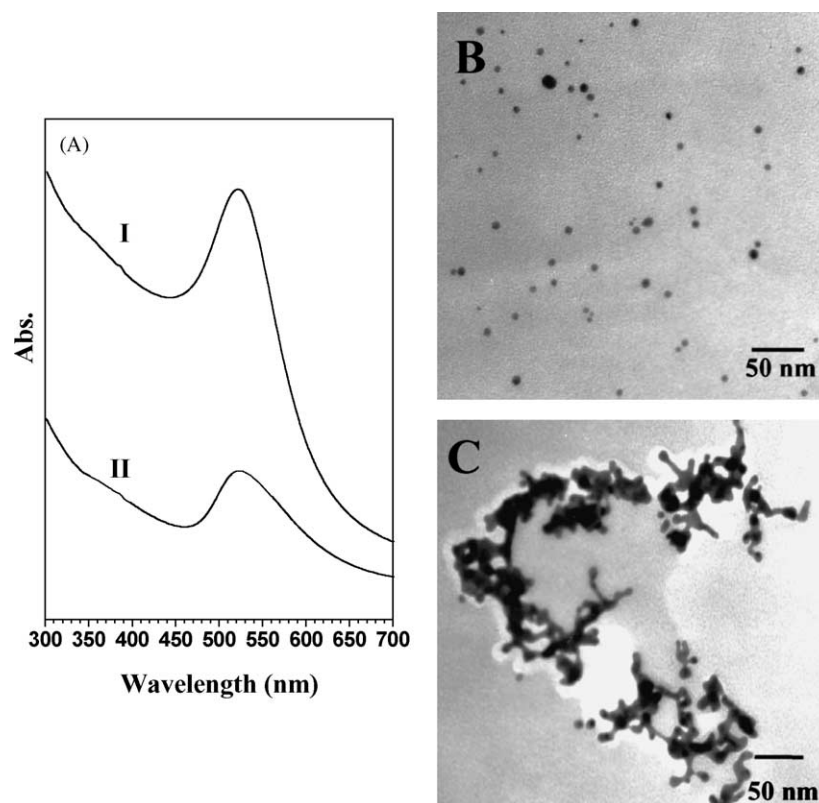


Fig. 1. (A) UV–vis spectra of Au@C₁₆TMAB (curve I) and Au@C₁₂TMAB (curve II), (B) TEM micrograph of Au@C₁₆TMAB, and (C) TEM micrograph of Au@C₁₂TMAB.

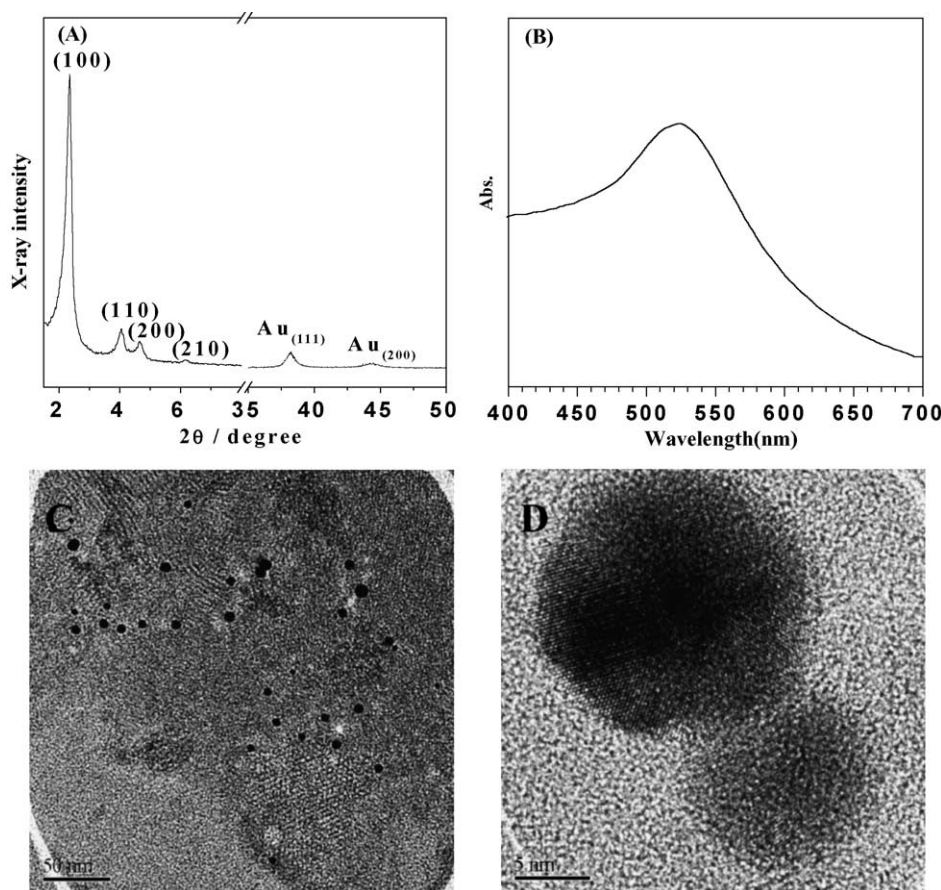


Fig. 2. (A) XRD patterns of calcined Au@MCM-41 prepared with C_{16} TMAB as template and undergone 6 h hydrothermal reaction, (B) diffuse-reflectance UV-vis spectra of Au@MCM-41, (C) and (D) microtoned HR-TEM images of Au@MCM-41.

at higher angle of 38.4° and 44.6° indicate the Au nanoparticles. Because the high-angle peaks are broader than those of bulk gold, it suggests that the Au particles are nanometer dimension. Fig. 2B displays the diffuse-reflectance UV-vis spectrum of Au@MCM-41. The absorption band at about 510 nm suggests again that Au particles remain in nanosize after high-temperature calcination [18].

To verify that Au nanoparticles were embedded within the mesoporous matrixes rather than just attached on the outer surface of mesostructured MCM-41 particle, the microtoned TEM images of Au@MCM-41 sample were taken. The TEM images (Fig. 2C and D) show that most of the gold nanoparticles are homogeneously embedded within the mesoporous aluminosilicate matrixes and the size of the Au nanoparticles is about 5–10 nm. Actually, there are very few Au particles attached on the peripherals of MCM-41 particles. Accordingly, the mesoporous matrixes can prevent a serious sintering of the embedded Au nanoparticles during calcination. Under the high-resolution TEM observation, the Au lattice fringes can be clearly observed. Since Au nanoparticles in the nanometer size range are known to have high catalytic activity for CO oxidation [1], therefore, CO oxidation was chosen as a test reaction for examining the activity of Au@MCM-41. Fig. 3A shows the CO conversion

over Au@MCM-41, prepared from different hydrothermal reaction time. It can be observed that Au@MCM-41 with 6 h hydrothermal treatment has the highest CO conversion of about 16.0%. However, the 0, 12, 24 h hydrothermally treated catalysts are only about 4, 8 and 2%, respectively. Thus, the samples prepared from a longer hydrothermal reaction time or without hydrothermal treatment possess lower catalytic activity for CO oxidation.

To understand the effect of the hydrothermal reaction time on the catalytic activity, the mesostructure and the dimension of Au nanoparticles in Au@MCM-41 after different hydrothermal time were examined. Fig. 3B displays the XRD patterns of Au@MCM-41 from different hydrothermal treatment time. It is obvious that Au@MCM-41 without hydrothermal treatment has only one broad peak at 2θ about 2.0° and two small peaks at high angle of 38.4° and 44.6° , which indicate a poor arrangement of mesostructure and fine Au nanoparticles. As the hydrothermal time is increased, it can be found the increase of peak intensities corresponding to (110), (200) and (210) crystal phases of low angle XRD, which suggests that the hexagonal-arranged mesostructure becomes more ordered and stable. In addition, the (111) and (200) peaks of Au lattice at high angle also turn sharper. According to Scherrer's equation, the Au

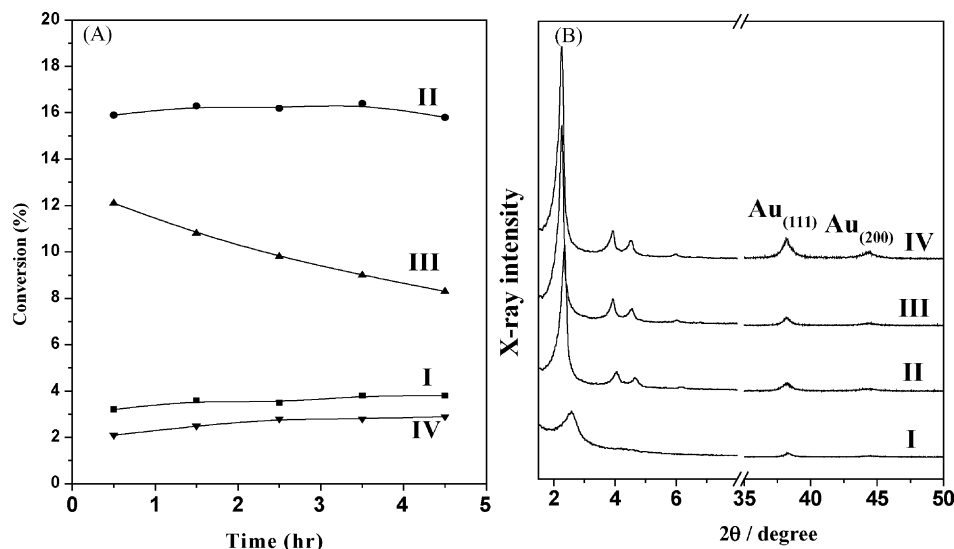


Fig. 3. (A) The conversion of CO oxidation over Au@MCM-41 catalysts, (B) XRD patterns of Au@MCM-41 prepared with C₁₆TMAB as template and undergone different hydrothermal reaction time for (I) 0 h, (II) 6 h, (III) 24 h, and (IV) 48 h.

nanoparticles embedded in the mesoporous structure also become larger due to sintering during longer hydrothermal treatment. Consequently, the hydrothermal treatment has dramatic influence on the mesostructures of MCM-41 and the sizes of Au nanoparticles, which affect the catalytic activity of the Au@MCM-41. Therefore, with a careful control on the hydrothermal time, the high-activity Au@MCM-41 catalyst with both stable mesostructure and proper-dimensioned Au nanoparticles can be obtained. Based on the catalytic results, the optimum hydrothermal time is around 6 h. Shorter hydrothermal time cannot make the mesostructure stable enough to withstand the 600 °C activation process. On the other hand, longer hydrothermal time induces a size increase of Au, and thus reduces the activity of Au nanoparticles.

In order to enhance the catalytic activity of Au@MCM-41, the loading of the Au nanoparticles within the aluminosil-

icate mesostructure should be increased. For comparison, CO conversions catalyzed by Au@MCM-41 from our previous research [11] are summarized in the following. It was found that the catalytic activity increased with the Au contents, and it reached a maximum at Au/SiO₂ = 8.0%. When Au/SiO₂ was larger than 8.0%, the catalytic activity decreased (Fig. 4A-I). This decrease of reaction activity at high Au content could be resulted mainly from the blocking of the nanochannels in the micron-sized MCM-41 aluminosilicates matrixes. This is because a long mesoporous channel might contain more than one Au nanoparticle, and thus the inner Au nanoparticles are not easily accessible to the CO and O₂ molecules for the reaction. It is reasonably postulated that only the Au nanoparticles at the outer part of the channel within Au@MCM-41 micro-particles are effective for the reaction. Thus, the micron-sized Au@MCM-41

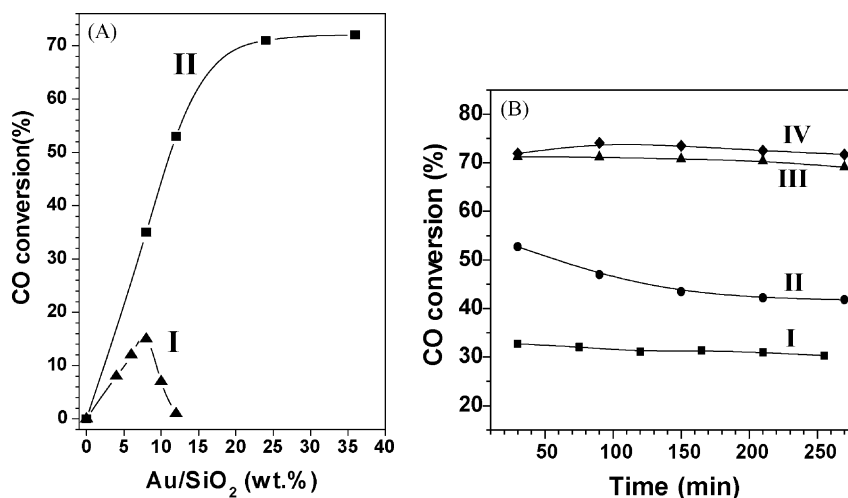


Fig. 4. (A) CO conversion over (I) Au@MCM-41 and (II) Au@nanoMCM-41 with different Au loading. The data of curve I are from Ref. [11], (B) CO conversion over Au@nanoMCM-41 with different Au loading(Au/SiO₂, *r*) vs. reaction time at 80 °C, (I) *r* = 8%, (II) *r* = 12%, (III) *r* = 24%, and (IV) *r* = 36%.

catalysts possessed relatively lower activity for CO oxidation at higher Au content (>8.0 wt.%).

To design a high-performance Au@MCM-41 catalyst, the accessibility of the Au nanoparticles is extremely important. For the linear channel system of MCM-41, this is particularly crucial. Basically, high accessibility of the nanochannels can be achieved effectively by reducing the domain size of the mesoporous aluminosilicate matrixes. In our previous report [11], it has been presented that MCM-41 (micron-sized) with a lot of void defects (~20 nm) can be synthesized and the extent of voids can be controlled during synthesis. Within this MCM-41 the channels become more effectively interconnected. Therefore for dehydrogenation of ethylbenzene to styrene, a better catalytic result was obtained from this catalyst [19].

In this paper, a different approach for achieving better catalytic results is applied. It is by making nanosized MCM-41 such that the channels length is very short in each particle. The method for the preparation relies on fast nucleation and quenching the growth of the mesoporous silica. Therefore, a fast-neutralization process was carried out to produce Au@nanoMCM-41. Fig. 5A shows that Au@nanoMCM-41 has only two broad XRD peaks at low

angle range of 1.5° – 4.0° and two peaks at high angle of 38.4° and 44.6° . From TEM image (Fig. 5B) one can see that the MCM-41 particles are very small, generally in the 30–50 nm range. Although the nanoparticles of MCM-41 are sticking together, the high inter-particle (textural porosity) space makes the nanochannels easily accessible. Besides, it is clear that the Au nanoparticles are dispersed homogeneously within or attached on the nanosized mesoporous aluminosilicate matrix, and the Au nanoparticles are mostly <10 nm. Under high-resolution (image not shown here) one can obviously see that the nanochannels of the mesoporous aluminosilicate are in a worm-like arrangement rather than the hexagonal packing of MCM-41. These TEM observation results are consistent with the broad XRD peaks at low angle, and the apparent absorption band at 520 nm in the diffuse-reflectance UV–vis spectrum (Fig. 5C) indicates nanosized gold. From these data, it is concluded that gold nanoparticles can be incorporated successfully within the nanosized mesoporous silica.

It should be noticed the sizes of Au nanoparticles are obviously bigger than the nanochannels of MCM-41, but not much bigger. In the synthesis, the initial surfactant-protected Au nanoparticles are already a little larger than 3 nm. The

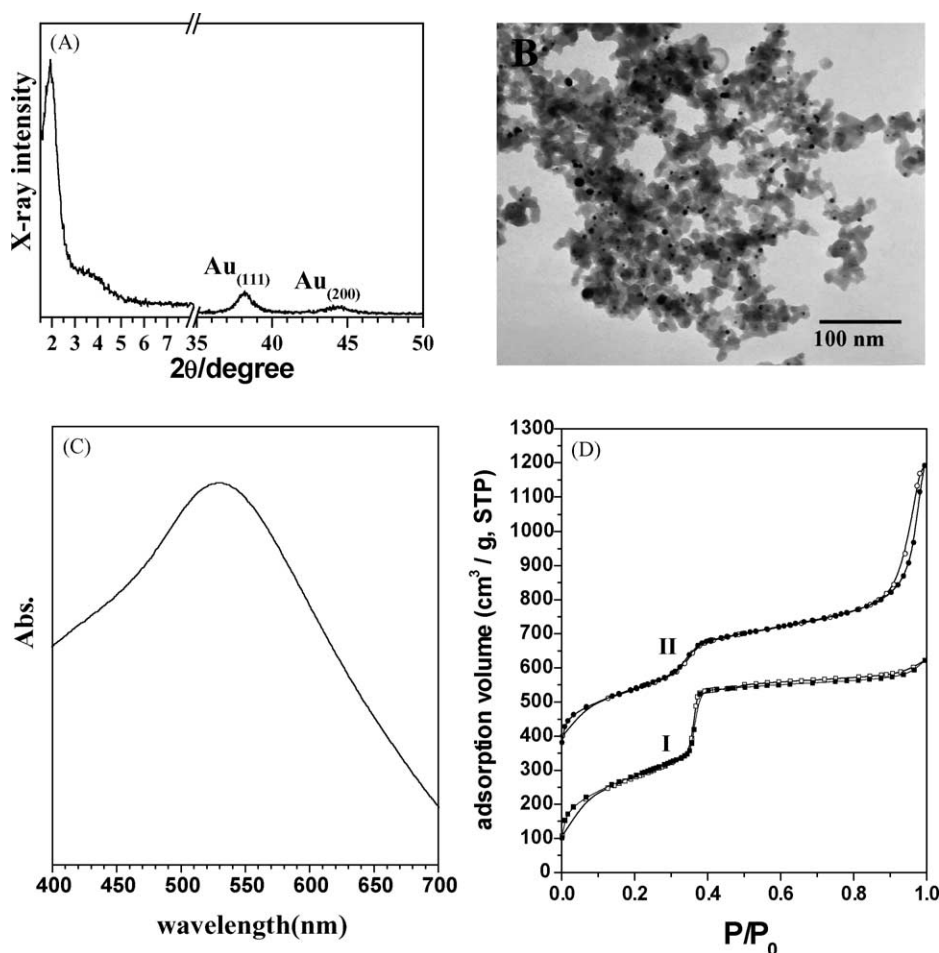


Fig. 5. (A) XRD pattern, (B) TEM micrograph, (C) diffuse-reflectance UV–vis spectra of Au@nanoMCM-41, and (D) N_2 adsorption–desorption isotherms from Au@MCM-41 (curve I) and Au@nanoMCM-41 (curve II).

hydrothermal and calcinations steps are both conducive towards agglomeration and sintering of the Au nanoparticles. The interaction between Au and silica surface has been generally considered as weak, and thus sintering of Au would be easy. This is in fact one of the reason Au deposited on silica is not a good catalyst. One tends to obtain much larger Au particle if the silica surface is flat. In our system, the embedding of the Au nanoparticles (bigger than channels) makes the movement of the Au particles less easy. So our Au nanoparticles, though a little bigger, are still very small. This may be the reason our Au@MCM-41 is catalytically more active.

The isotherms of nitrogen adsorption–desorption from Au@MCM-41 and Au@nanoMCM-41 are shown in Fig. 5D. Relative to the adsorption from Au@MCM-41 (curve I), the adsorption from Au@nanoMCM-41 (curve II) displays a very large additional adsorption (vertical rise) at P/P_0 near 0.9 (Fig. 5D). This large additional adsorption is due to the textural porosity caused by the packing between the nanosized particles. Due to the existence of this large textural porosity, the Au nanoparticles in the mesopores are more accessible to the reactants (CO and air) and the permeability for the reactants within Au@nanoMCM-41 must be high.

With the high accessibility and permeability, the nanosized Au@nanoMCM-41 would be a high-performance catalyst for CO oxidation. As expected, the Au@nanoMCM-41 shows significantly higher CO conversion than micron-sized Au@MCM-41 at the same Au/SiO₂ loading (Fig. 4A-II). It is found that unlike the micron-sized mesoporous aluminosilicate matrix, the CO conversion over Au@nanoMCM-41 increases with the increase of the Au/SiO₂ ratio, and level off around 70% at Au/SiO₂ = 24 wt.%. There is no activity drop with the increase of Au content, due to high accessibility of the Au@nanoMCM-41. The highest CO conversion is achieved to about 75% at 80 °C. Also, Fig. 4B shows that the catalytic activities are fairly stable over an extended period. Thus, the gold nanoparticles embedded within nanosized mesoporous silica show high activity for CO oxidation reaction. It is noticed that the catalytic activity of gold nanoparticle depends on the kind of oxide support. [20] Silica, lacking redox property, is generally regarded as a poor support for the active sites for CO oxidation. The high CO conversion observed in this work is in fact somewhat surprising. However, the methods developed in this work should be general. Therefore, it opens up a whole new vista of dispersed catalysts design that one can support nanocrystalline materials, like metal nanoparticles, on the other more effective supports, such as TiO₂ [21].

4. Conclusion

The quaternary ammonium salt C₁₆TMAB is capable of being protecting agents for gold nanoparticles. The aqueous

Au@C₁₆TMAB solution can serve as mesoporous structure templates, and the Au nanoparticles containing mesoporous aluminosilicates can be synthesized conveniently and reproducibly. The gold nanoparticles are uniformly incorporated in the mesoporous matrixes. By reducing the domain size of mesoporous aluminosilicates from micrometer to nanometer, the catalytic activity of aluminosilicates supported gold nanoparticles increases remarkably. The nanosized mesoporous silica could tolerate very high loading of gold nanoparticles up to 36 wt.%. The nanosized mesoporous materials have significant capacity to support active species and possess high permeability of reactants for catalytic reaction. Therefore at the same loading of nanogold, the catalytic activity of nanosized Au@nanoMCM-41 for CO oxidation is much higher than that of micron-sized Au@MCM-41.

Acknowledgements

This work was supported from the program of Academy Excellence sponsored by Ministry of Education in Taiwan.

References

- [1] A.I. Kozlov, A.P. Kozlov, H. Liu, Y. Iwasawa, *Appl. Catal. A: Gen.* 182 (1999) 9.
- [2] M. Haruta, M. Date, *Appl. Catal. A: Gen.* 222 (2001) 427.
- [3] G.C. Bond, *Catal. Today* 72 (2002) 5.
- [4] H. Sakurai, M. Haruta, *Catal. Today* 29 (1996) 361.
- [5] M. Valden, X. Lai, D.W. Goodman, *Science* 281 (1998) 1647.
- [6] M. Haruta, *Catal. Today* 36 (1997) 153.
- [7] A. Wolf, F. Schüth, *Appl. Catal. A: Gen.* 226 (2002) 1.
- [8] M.M. Schubert, V. Plzak, J. Garche, R.J. Behm, *Catal. Lett.* 76 (2001) 143.
- [9] L. Guzzi, G. Peto, A. B. K. Frey, O. Geszti, G. Molnar, C. Daroczi, *J. Am. Chem. Soc.* 125 (2003) 4332.
- [10] J.J. Pietron, R.M. Stroud, D.R. Rolison, *Nano Lett.* 2 (2002) 545.
- [11] H.P. Lin, Y.S. Chi, J.N. Lin, C.Y. Mou, B.Z. Wan, *Chem. Lett.* (2001) 1116.
- [12] D.R. Rolison, *Science* 299 (2003) 1698.
- [13] M. Okumura, S. Tsubota, M. Iwamoto, M. Haruta, *Chem. Lett.* (1998) 315.
- [14] A. Ghosh, C.R. Patra, P. Mukherjee, R. Kumar, M. Sastry, *Micropor. Mesopor. Mater.* 58 (2003) 201.
- [15] H. Zhu, B. Dai, S.H. Overbury, *Langmuir* 19 (2003) 3974.
- [16] H.P. Lin, C.P. Tsai, *Chem. Lett.* 32 (2003) 1092.
- [17] J.J. Storhoff, A.A. Lazarides, R.C. Mucic, C.A. Mirkin, R.L. Letsinger, G.C. Schatz, *J. Am. Chem. Soc.* 122 (2000) 4240.
- [18] P. Mukherjee, C.R. Patra, A. Ghosh, R. Kumar, M. Sastry, *Chem. Mater.* 14 (2002) 1678.
- [19] S.T. Wong, H.P. Lin, C.Y. Mou, *Appl. Catal. A* 198 (2000) 103.
- [20] M.M. Schubert, S. Hackenberg, A.C. van Veen, M. Muhler, V. Plzak, R.J. Behm, *J. Catal.* 197 (2001) 113.
- [21] M. Anpo, M. Takeuchi, *J. Catal.* 216 (2003) 505.